

Mei Xiao, ChenChen Zou
The Jackson Laboratory
Farmington, CT, USA

Keith Sheppard, Mark P. Krebs
The Jackson Laboratory
Bar Harbor, ME, USA

Abstract—Optical coherence tomography (OCT) is an important tool for analyzing small animal models of ocular disease. As OCT image quality and downstream analysis are affected by speckle noise, we have developed an algorithm to average multiple OCT volume datasets obtained by repeatedly scanning the same mouse eye. Here, we address the pulsatile movement of ocular tissue along an axis parallel to the OCT light path, which compromises the quality of the registered and averaged images. As a refinement of the algorithm, we show that image quality is improved by restricting the iterative alignment process to increments along the y image axis, which parallels the OCT light path.

Index Terms—Optical coherence tomography, *en face* OCT, segmentation, alignment, registration, mouse retina

I. Introduction

The application of noninvasive imaging methods to small animal models of human disease has proven to be invaluable for understanding disease pathogenesis. Optical coherence tomography (OCT) is a non-invasive and high-resolution method that has been widely applied in this field, particularly in the eye [1], [2]. For example, using OCT to capture image volumes, large amounts of information from the mouse retina and nearby tissues can be retrieved in a short time frame (see Fig. 1, 2 and 3). This detailed image data allows researchers to build and test hypotheses and models intuitively and quantitatively. For these reasons, OCT imaging may aid ocular phenotyping in large-scale high-throughput efforts, such as the Knockout Mouse Phenotyping Project (KOMP²) and International Mouse Phenotyping Consortium (IMPC), which aim to create a functional catalog of >20,000 mouse genes.

To analyze retinal phenotypes or disease patterns, it is common to detect and precisely separate (segment) each layer in the retinal image and determine its thickness [3], [4], [5]. Image segmentation may also be useful to quantify changes in lesions and blood vessels during disease progression. In large-scale research projects, hundreds or thousands of mice are scanned multiple times. Developing automated or semi-automated segmentation algorithms would improve opportunities to exploit the full utility of OCT datasets. However, OCT images suffer from speckle noise (see Fig. 1, 2), and this noise is the fundamental barrier to segmenting retinal layers [2]. Moreover, speckle noise inherently exists in OCT technology because of limited spatial-frequency bandwidth during the signal measurement.

Most segmentation pipelines include a pre-processing step to try to remove different types of noise. Various de-noising

algorithms have been used to pre-process the OCT images. 2D or 3D spatial image filters such as median filter, mean filter, Gaussian kernel filter, directional filter and wavelet shrinkage, etc., have been applied to enhance OCT images. However speckle noise in OCT is a random phenomenon, and linear filter algorithms usually suppress this type of noise at the cost of softening the images and losing detail [3], [4], [5], [6], [7]. Signal averaging, in which a set of replicate measurements is averaged, can increase the signal-to-noise ratio efficiently. This technique is robust for removing random speckle noise [7]. Therefore, to allow signal averaging, we refined an algorithm to process multiple OCT volume scans of the same mouse retina acquired in rapid succession. The resulting OCT image stacks are registered and averaged based on intensity to create a clearer stack with more visible tissue details. However, ocular movements during data acquisition can introduce image artifacts that compromise the quality of the averaged image stack. By analyzing the image stacks, we found that constraining a key registration step to iterate in a single direction successfully reduced motion-associated artifacts.

II. Methods

We analyzed ten retinal OCT volume datasets scanned successively from a single mouse eye using an R2200 ultrahigh resolution spectral domain OCT system (Bioptigen, Raleigh, NC) on a 32-bit Windows operating system. Mice were anesthetized prior to and during the scanning and the interval between scans was within five seconds. The acquisition was nonisotropic, with 1000 A-scans per B-scan and 100 B-scans over a 1.4 mm-diameter retinal area. The original datasets were saved as *.oct files, a proprietary format generated by the InVivoVue software (Bioptigen), and converted to *.tif format with a custom Java application (OCTToTIFF) based on an OCT Reader plugin provided by Bioptigen. The pixel dimension of the converted image stacks is $1000 \times 1024 \times 100$ (xy by z slices). Files were analyzed in ImageJ/Fiji [8], [9].

The OCT Volume Averager algorithm we are developing is based on ImageJ/Fiji plugins. Briefly, the algorithm accesses replicate OCT volume scans in a user-designated directory, automatically converts files from *.oct to *.tif format and crops the images according to user input. The n^{th} image slice is then read from all replicate image stacks acquired from a single eye, and TurboReg [10] is used to register these slices, which are then averaged based on intensity. The resulting averaged image stack is aligned with StackReg [10], a plugin that aligns images within a single stack and relies on the TurboReg registration algorithm. OCT Volume Averager is being refined as an ImageJ/Fiji plugin and as a standalone Java application.

III. Results and Discussion

To examine the need for within-stack registration, image slices from a single OCT volume scan of a mouse retina were displayed in ImageJ (each slice corresponds to a B-scan from the OCT volume dataset). Subtle vertical movements were observed to occur repeatedly, as seen by comparing slices from the image stack (Fig. 1A and B). Movements of the retina and surrounding tissue possibly due to heartbeat and breathing may account for these relatively small changes in image position [5], [11]. Artifacts due to human operation and device setup, etc., may also have contributed to the observed movement [12]. The repeated shifts were distinct from displacements between the ends and middle of the scan (Fig. 1A and C), which result from imperfect alignment of the optical path of the instrument with that of the eye, resulting in a tilting of the retina with respect to the imaging beam, or from incomplete adjustment of the instrument to correct for the curvature of the posterior eye.

The ImageJ/Fiji plugin StackReg registers slices of an image stack [10]. To demonstrate the utility of StackReg on OCT volume scans of the retina, the image stack was converted to an *en face* orientation using the Stack>Reslice function of ImageJ. Single *en face* slices exhibited horizontal banding artifacts that reflect vertical movement during acquisition, as described above (see Fig. 2A). For comparison, StackReg was applied to the image stack, and the aligned image stack was then also converted into an *en face* orientation (see Fig. 2B). Comparison of these images showed that StackReg reduced the horizontal banding artifacts caused by ocular movement.

Integrating StackReg alignment into OCT Volume Averager plugin is under development. To demonstrate the improvement in image quality achieved by StackReg, we ran the plugin with or without deploying StackReg. OCT Volume Averager reads the n^{th} image slice from all replicates, uses TurboReg to align those slices and averages them based on intensity, yielding a new image stack. A single *en face* slice of the results obtained by averaging replicate scans without StackReg is shown in Fig. 3A. The image quality is much better than in the corresponding stack without averaging (compare with Fig. 2), but horizontal bands remain. After applying StackReg to the averaged image stack, more details are visible (Fig. 3B) and horizontal banding is reduced.

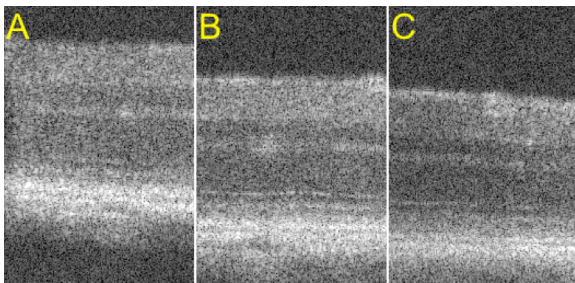


Fig. 1. Vertical displacement of individual slices (B-scans) in an image stack from an OCT volume scan. A) Slice 1. B) Slice 11. C) Slice 63. Cropped images from the same x range are shown.

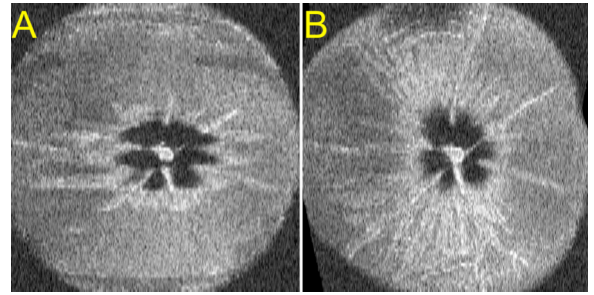


Fig. 2. A) *En face* view of a slice from a single OCT volume dataset without alignment. B) Corresponding slice with stack alignment.

However, the expected circular shape of the image is skewed and appears ovoid. This could be due to the fact that the automatic alignment algorithm in StackReg does not compensate for the systematic shifting errors effectively.

We sought to understand the behavior of the image movement to develop an alignment approach that did not result in a skewed image. We therefore examined the displacement of each slice in all of the replicate OCT volume scans. Image stacks were opened in ImageJ and a median filter was applied first to smooth the images. Intensity was then thresholded manually to convert the whole stack from 8-bit gray scale image into a binary black and white image. The retinal tissue area was indicated as white pixels and the background as black. We chose seven uppermost white pixels (closest to the vitreous) corresponding to an x value between 200-800 pixels with a step of 100 pixels. The median y value of those seven pixels was taken as the upper limit of the retinal tissue. The location of this limit in each slice of ten replicate image stacks is displayed in Fig. 4A. Each image stack shows a slightly different but mostly similar shifting pattern. We applied the same procedure to the averaged and StackReg aligned image stack, as shown in Fig. 4B, *dashed line*. By comparing the shifting range in Fig. 4, A and B, we can see that StackReg, as an automatic registration program, tried to find the vertical shift and compensate for that. The shifting range in Fig. 4B is much smaller than the shifting range in Fig. 4A. However, the automated alignment program stopped once reached the iteration limit or the intensity threshold. This could explain the skewed averaged image observed in Fig. 3B.

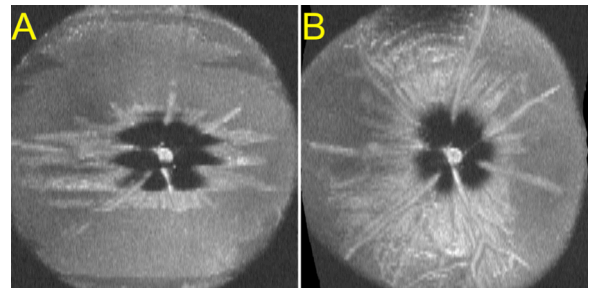


Fig. 3. A) Single *en face* slice from an OCT image stack after multiple stack image averaging. B) Single slice of the same dataset after multiple stack image averaging and alignment.

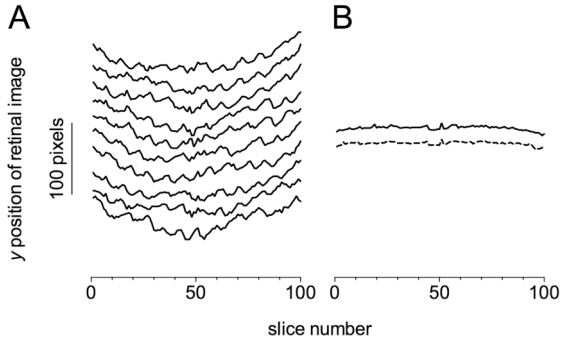


Fig. 4. A) Displacement of OCT retinal images along the y -axis with slice number in replicate image stacks acquired from a single eye. B) Reduced displacement of the averaged and aligned image stacks using OCT Volume Averager algorithm with (solid line) or without (dashed line) limiting StackReg to fit in the y dimension.

To average all the image stacks and also keep the original retina shape as much as possible for further comparison and measurements, we decided to compensate only the vertical image shifts. As StackReg relies on TurboReg [10], we created a modified implementation of TurboReg, named TurboRegY, which allows only vertical shifts for the transformation.

Registration in TurboReg employs an automatic algorithm to calculate the integrated square difference of pixel intensity values as a measure of the similarity of two images. The plugin uses f_R as the intensity for the reference image, and f_T as the intensity for the test image. TurboReg then tries to find a transformation parameterized by p that can minimize the following criterion:

$$\|f_R(x) - Q_p(f_T(x))\|^2 \quad (1)$$

TurboReg can handle images with different color scheme and can perform various transformations. OCT image stacks are 8-bits grayscale. To keep the retina shape, we chose to use only 2D translation to align two images. Thus, to minimize the value in equation (1), after each iteration, the translation parameter p will translate the pixel X (with coordinates x, y) into a new location X' (with coordinates x', y').

$$X' = \begin{bmatrix} x' \\ y' \end{bmatrix} = \begin{bmatrix} x \\ y \end{bmatrix} + \begin{bmatrix} p_x \\ p_y \end{bmatrix} \quad (2)$$

In the modified TurboRegY algorithm, using 2D translation on 8-bit grayscale images, we changed the routine to update the parameter p . After every iteration towards minimizing the equation (1), the translation parameter p will update only the y coordinate for pixel X as shown in the following equation.

$$X' = \begin{bmatrix} x' \\ y' \end{bmatrix} = \begin{bmatrix} x \\ y \end{bmatrix} + \begin{bmatrix} 0 \\ p_y \end{bmatrix} \quad (3)$$

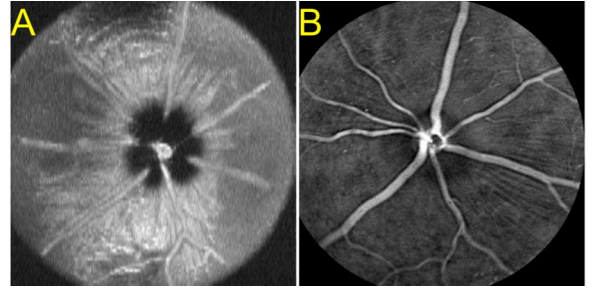


Fig. 5. A) Mouse eye *en face* view after multiple stack image averaging and alignment using the modified StackReg implementation in the OCT Volume Averager algorithm, in which the alignment transformation is limited to the vertical y -axis. B) Brightfield fundus image of the same eye processed to reveal the superficial retinal blood vessels, scaled and cropped to match A.

In OCT Volume Averager, TurboRegY is invoked only when called by StackReg to align the image stack averaged from all replicate scans; the unmodified TurboReg is used for the earlier registration steps. The *en face* view of the averaged and aligned image shows little sign of skewing (Fig. 5A) and the quality of this modified registration is similar to that of the original StackReg implementation (compare with Fig. 3B). The visual differences of the averaged images confirmed that the vertical shifts caused by the animals' physiological motion should be restricted during the image registration step. The retinal blood vessels shown in Fig. 5A closely match those highlighted by brightfield fundus imaging of the same eye (Fig. 5B), providing qualitative evidence that the algorithm is performing accurately. We also analyzed the vertical shifting pattern of the averaged and aligned image stack using the modified StackReg, which used our TurboRegY implementation. The vertical shifting pattern is shown in Fig. 4B, solid line. It is very close to the averaged and aligned image stack using the original StackReg implementation. This suggests that the overcompensation of the horizontal shifts from the original StackReg source code is the main reason for the skewed image stack. In the future image analysis of OCT image stacks it may be necessary to pay more attention to additional noise introduced by generic optimization algorithms.

IV. Conclusion

OCT is an efficient noninvasive 3D imaging technology for analyzing mouse models of ocular disease to characterize pathological features and to evaluate the effects of potential treatments. Although commercial instruments provide high quality OCT volume data, further quality improvement by data averaging is expected to enhance the qualitative and quantitative assessment of ocular disease progression. As part of an ongoing refinement of OCT Volume Averager, an ImageJ-based registration and averaging algorithm for processing replicate OCT volume scans in the eye, we identified vertical displacement of B-scan images during the acquisition process as a prominent source of image artifacts. Application of TurboRegY, a modified version of TurboReg restricted to registration in the y dimension, improved the output of this algorithm.

Fundus images from other modalities, such as brightfield imaging, offer the possibility to segment retinal blood vessels clearly and completely from the original image stack. Therefore, besides the intensity based global registration, it may be possible to use the segmented structure to apply feature-based registration to align and average the OCT image stacks. After extracting features of our interest, 3D visualization could also be used to examine further the results of averaging the aligned multiple image stacks and allow us to determine the sources of various noise. Although more sophisticated automated 2D/3D registration programs may further improve the averaging of OCT volume stacks, it is likely that pre-processing of image stacks to compensate for the vertical shift in each stack will continue to be necessary for optimal image quality.

Acknowledgment

The authors thank Wanda Hicks for technical assistance with live mouse imaging and Patsy Nishina for providing laboratory space, research animals and access to instruments. This research was supported by funds from NIH grants EY016501 (to Patsy M. Nishina) and CA34196 (in support of core services at The Jackson Laboratory).

References

- [1] P. Li, Z. Ding, Y. Ni, B. Xu, C. Zhao, Y. Shen, C. Du, and B. Jiang, "Visualization of the ocular pulse in the anterior chamber of the mouse eye in vivo using phase-sensitive optical coherence tomography," *Journal of Biomedical Optical*. 2014, vol. 19(9).
- [2] R. Kafieh, H. Rabbanj, and S. Kermani, "A review of algorithms for segmentation of optical coherence tomography form retina," *Journal of Medical Signals and Sensors*. 2013, vol. 3(1).
- [3] L.R. Ferguson, J.M. Dominguez, S. Balaiya, S. Grover and K.V. Chalam, "Retinal Thickness Normative Data in Wild-Type Mice Using Customized Miniature SD-OCT", 2013, PLoS ONE 8(6): e67265.
- [4] E.J. Knott, K.G. Sheets, Y. Zhou, W.C. Gordon and N.G. Bazan, "Spatial correlation of mouse photoreceptor-RPE thickness between SD-OCT and histology", *Exp Eye Res*. 2011 92(2).
- [5] A. Berger, S. Cavallero, E. Dominguez, P. Barbe, M. Simonutti, et al. "Spectral-Domain Optical Coherence Tomography of the Rodent Eye: Highlighting Layers of the Outer Retina Using Signal Averaging and Comparison with Histology". *PLoS ONE*, 2014 9(5)
- [6] Wim Van Drongelen. "Signal Processing for Neuroscientists." Academic Press, 2006.
- [7] C. Maduro, P. Serranho, T. Santos, P. Rodrigues, J. Cunha-Vaz, R. Bernardes. OCT Noise Despeckling "Using 3D Nonlinear Complex Diffusion Filter". *Technologies for Medical Sciences, Lecture Notes in Computational Vision and Biomechanics*. 2012.
- [8] Schneider C.A., Rasband W.S., Eliceiri K.W. "NIH Image to ImageJ: 25 years of image analysis". *Nature Methods*. July 9(7): 671-675. 2012
- [9] Schindelin J., Arganda-Carreras I., Frise E., Kaynig V., Longair M., Pietzsch T., Preibisch S., Rueden C., Saalfeld S., Schmid B., Tinevez J., White D.J., Hartenstein V., Eliceiri K., Tomancak P., Cardona A. "Fiji: an open-source platform for biological-image analysis". *Nature Methods* 9, 767-682. 2012.
- [10] Thevenaz P., Ruttimann U.E., Unser M. "A pyramid approach to subpixel registration based on intensity". *IEEE Transactions on Image Processing*. Vol. 7, No. 1, January 1998
- [11] J. Chhablani, T. Krishnan, V. Sethi, and I. Kozak, "Artifacts in optical coherence tomography". *Saudi Journal of Ophthalmology*. 2014 28(2)
- [12] I.V. Larina, K.V. Larin, M.J. Justice and M.E. Dickinson, "Optical Coherence Tomography for live imaging of mammalian development". *Curr Opin Genet Dev*. 2011 21(5)